

Nucleon mass, sigma term and lattice QCD¹

Massimiliano Procura^{a,b}, Thomas R. Hemmert^a and Wolfram Weise^{a,b}

^a *Physik-Department, Theoretische Physik
Technische Universität München, D-85747 Garching, Germany
(Email: themmert@physik.tu-muenchen.de)*

^b *ECT*, Villa Tambosi, I-38050 Villazzano (Trento), Italy
(Email: weise@ect.it, procura@ect.it)*

Abstract

We present a study on the quark mass dependence of the nucleon mass M_N and an extrapolation of this observable to two-flavor lattice QCD results in the framework of relativistic baryon chiral perturbation theory up to order p^4 . Already at leading-one-loop order we obtain a good chiral extrapolation function and we demonstrate that the next-to-leading one loop corrections are reasonably small. From the p^4 extrapolation we find $M_N = 910 \pm 70$ MeV at the physical value of the pion mass. Furthermore, utilizing the same parameters determined in our numerical analysis of M_N we also examine the quark mass dependence of the pion-nucleon sigma term σ_N , resulting in $\sigma_N = 53 \pm 8$ MeV at the physical value of the pion mass.

¹Work supported in part by BMBF and DFG

1 Introduction and framework

Lattice QCD on one side and chiral effective field theory, on the other, are progressively developing as important tools to deal with the non-perturbative nature of low-energy QCD and the structure of hadrons [1]. The merger of both strategies has recently been applied to extract physical properties of hadrons—such as the nucleon—from lattice QCD simulations. Of particular interest in such extrapolations is the detailed quark mass dependence of nucleon properties. Examples of recent extrapolation studies concern the nucleon mass [2, 3], its axial vector coupling constant and magnetic moments [4, 5], form factors [6] and moments of structure functions [7].

Accurate computations of the nucleon mass with dynamical fermions and two active flavors are now possible [8, 9, 10]. However, the masses of u - and d -quarks used in these evaluations exceed their commonly accepted small physical values by typically an order of magnitude. It is at this point where chiral effective field theory methods are useful - within limitations discussed extensively in refs. [2, 3] - in order to interpolate between lattice results, actual observables and the chiral limit ($m_{u,d} \rightarrow 0$). In this paper we explore the capability of such an approach for extracting the nucleon mass and the pion-nucleon sigma term.

The nucleon mass is determined by the expectation value $\langle N | \Theta_\mu^\mu | N \rangle$ of the trace of the QCD energy-momentum tensor [11],

$$\Theta_\mu^\mu = \frac{\beta(g)}{2g} G_{\mu\nu} G^{\mu\nu} + m_u \bar{u}u + m_d \bar{d}d + \dots , \quad (1)$$

where $G^{\mu\nu}$ is the gluonic field strength tensor, $\beta(g)$ is the beta function of QCD and $m_q \bar{q}q$ with $q = u, d \dots$ are the quark mass terms (we omit here the anomalous dimension of the mass operator, as in [12]). So the physical nucleon mass M_N can be expressed as

$$M_N = M_0 + \sigma_N \quad (2)$$

in terms of its value in $SU(2)_f$ chiral limit

$$M_0 = \langle N | \frac{\beta}{2g} G_{\mu\nu} G^{\mu\nu} + \dots | N \rangle \quad (3)$$

(where the dots refer to possible contributions from heavier quarks, other than u and d), and the sigma term defined as

$$\sigma_N = \sum_{q=u,d} m_q \frac{dM_N}{dm_q} = \langle N | m_u \bar{u}u + m_d \bar{d}d | N \rangle, \quad (4)$$

with $\langle N | N \rangle = 1$. The quark mass dependence of M_N translates into a dependence on the pion mass: $m_\pi^2 \sim m_q$ at leading order. We pursue this connection in the symmetry breaking part of the chiral effective Lagrangian.

The framework of our study will be relativistic $SU(2)_f$ baryon chiral perturbation theory (BChPT) as described in ref.[13]. The effective Lagrangian required for our analysis of the nucleon mass up to $\mathcal{O}(p^4)$ is

$$\mathcal{L} = \mathcal{L}_N^{(1)} + \mathcal{L}_N^{(2)} + \mathcal{L}_N^{(4)} + \mathcal{L}_\pi^{(2)} \quad (5)$$

with

$$\begin{aligned} \mathcal{L}_N^{(1)} &= \bar{\Psi} (i\gamma_\mu D^\mu - M_0) \Psi + \frac{1}{2} g_A \bar{\Psi} \gamma_\mu \gamma_5 u^\mu \Psi, \\ \mathcal{L}_N^{(2)} &= c_1 \text{Tr}(\chi_+) \bar{\Psi} \Psi - \frac{c_2}{4M_0^2} \text{Tr}(u_\mu u_\nu) (\bar{\Psi} D^\mu D^\nu \Psi + \text{h.c.}) + \frac{c_3}{2} \text{Tr}(u_\mu u^\mu) \bar{\Psi} \Psi + \dots \\ \mathcal{L}_N^{(4)} &= e_{38} (\text{Tr}(\chi_+))^2 \bar{\Psi} \Psi + \frac{e_{115}}{4} \text{Tr}(\chi_+^2 - \chi_-^2) \bar{\Psi} \Psi \\ &\quad - \frac{e_{116}}{4} (\text{Tr}(\chi_-^2) - (\text{Tr}(\chi_-))^2 + \text{Tr}(\chi_+^2) - (\text{Tr}(\chi_+))^2) \bar{\Psi} \Psi + \dots \quad . \end{aligned} \quad (6)$$

In $\mathcal{L}_N^{(4)}$ we follow the notation of ref.[14]. Here $\mathcal{L}_\pi^{(2)}$ is the leading order pion Lagrangian including the mass term. The nucleon Dirac field is denoted by Ψ , and M_0 is the nucleon mass in the chiral limit. The axial field u^μ and the covariant derivative D^μ involve the chiral meson field $U(x) \in SU(2)$, and $\chi_\pm = u^\dagger \chi u^\dagger \pm u \chi^\dagger u$, $u^2 = U$ parametrizes the explicit chiral symmetry breaking through the quark masses; here $\chi = 2B\mathcal{M}$, where $\mathcal{M} = \text{diag}(m_u, m_d)$ and $B = -\langle \bar{q}q \rangle / f_\pi^2$ is the chiral condensate divided by the squared pion decay constant, both taken in the chiral limit. In the following we neglect isospin breaking effects.

2 Analytic results

2.1 $\mathcal{O}(p^3)$ Analysis

The leading order contribution to the shift of the nucleon mass from its value in the chiral limit comes from the explicit chiral symmetry breaking piece in $\mathcal{L}_N^{(2)}$ which drives the nucleon sigma term σ_N of Eq.(4). The next-to-leading order (NLO) contribution is represented by diagram (a) of Fig.1, with the πNN vertex generated by $\mathcal{L}_N^{(1)}$. We have evaluated the relevant one-loop integrals using the so-called infrared regularization method [13]. It represents a variant of dimensional regularization which handles one-loop integrals involving baryon propagators in a way consistent with chiral power-counting. The diagram (a) develops a divergence proportional to m_π^4 which has to be absorbed in contact terms which formally are of fourth order. We denote² the counter term structure that renders the $\mathcal{O}(p^3)$ contribution finite as $-e_1 m_\pi^4 \bar{\Psi} \Psi$. In the notation of ref.[14] it involves the coupling constant combination $e_1 = -(16e_{38} + 2e_{115} + 2e_{116})$ from $\mathcal{L}_N^{(4)}$.

Following the reasoning outlined here, the constraint to obtain a finite result at leading-one-loop order has effectively promoted a linear combination of p^4 couplings—denoted by

²Our coupling e_1 differs from convention of ref.[3] by a factor 4.

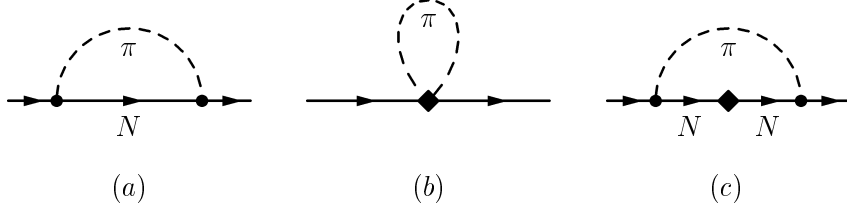


Figure 1: One-loop graphs of NLO (a) and NNLO (b, c) contributing to the nucleon mass shift. The solid dot denotes a vertex from $\mathcal{L}_N^{(1)}$, the diamond a vertex from $\mathcal{L}_N^{(2)}$.

e_1 —into the p^3 calculation. The resulting relativistic (renormalized) leading one-loop expression for the m_π dependence of M_N then reads:

$$\begin{aligned} M_N = & M_0 - 4c_1 m_\pi^2 + \left[e_1^r(\lambda) + \frac{3g_A^2}{64\pi^2 f_\pi^2 M_0} \left(1 - 2 \ln \frac{m_\pi}{\lambda} \right) \right] m_\pi^4 \\ & - \frac{3g_A^2}{16\pi^2 f_\pi^2} m_\pi^3 \sqrt{1 - \frac{m_\pi^2}{4M_0^2}} \left[\frac{\pi}{2} + \arctan \frac{m_\pi^2}{\sqrt{4M_0^2 m_\pi^2 - m_\pi^4}} \right]. \end{aligned} \quad (7)$$

Here $e_1^r(\lambda)$ is the finite (renormalization scale λ dependent) part of e_1 ,

$$e_1 = e_1^r(\lambda) + \frac{3g_A^2}{2f_\pi^2 M_0} L(\lambda) ,$$

and any ultraviolet divergences appearing in the limit $d \rightarrow 4$ are subsumed in

$$L(\lambda) = \frac{\lambda^{d-4}}{16\pi^2} \left[\frac{1}{d-4} - \frac{1}{2} (\ln(4\pi) + \Gamma'(1) + 1) \right].$$

For further discussion we expand the $\mathcal{O}(p^3)$ result Eq.(7) in powers of the pion mass and obtain

$$\begin{aligned} M_N = & M_0 - 4c_1 m_\pi^2 - \frac{3g_A^2}{32\pi f_\pi^2} m_\pi^3 \\ & + \left[e_1^r(\lambda) - \frac{3g_A^2}{64\pi^2 f_\pi^2 M_0} \left(1 + 2 \ln \frac{m_\pi}{\lambda} \right) \right] m_\pi^4 \\ & + \frac{3g_A^2}{256\pi f_\pi^2 M_0^2} m_\pi^5 + \mathcal{O}(m_\pi^6). \end{aligned} \quad (8)$$

Note that the sum of the first three terms in this formula coincides with the well-known leading one-loop expression for M_N of Heavy Baryon Chiral Perturbation Theory (HBChPT), as expected in the infrared regularization approach [13]. We further remark that from Eq.(8) one can also deduce that the counterterm e_1 of Eq.(7), which in relativistic baryon ChPT is required for renormalization purposes, is equivalent to the counterterm introduced in [3]

regulating the short distance behaviour in HBChPT for large pion masses. We therefore conclude that our analysis of $M_N(m_\pi)$ does not suffer from the problems discussed in [3]. Finally, we would like to point out that Eq.(8) also shows that all the terms beyond the leading c_1 contribution to the nucleon mass are part of the same chiral order p^3 . From the viewpoint of relativistic baryon ChPT the large fluctuations in the chiral extrapolation function discussed in [2] can therefore be understood to arise from a choice to expand Eq.(7) up to too low powers in m_π as in Eq.(8), instead of keeping the full expression Eq.(7).

2.2 $\mathcal{O}(p^4)$ Analysis

Let us now focus on the next-to-NLO (NNLO) contribution to the pion mass dependence of the nucleon mass. This involves also graphs (b) and (c) in Fig.1 which include vertices generated by $\mathcal{L}_N^{(2)}$. The tadpole (b) develops a divergence proportional to m_π^4 that can be absorbed in e_1 . On the other hand diagram (c) produces, in principle, an infinite string of different divergent terms proportional to m_π^{2n} with $n \geq 3$. Thus in order to avoid having to deal with an uncontrollably large number of counterterms, we decide to truncate the chirally expanded formula at $\mathcal{O}(m_\pi^6)$ ³. Up to this power no counterterms other than e_1 are required for a finite result. At $\mathcal{O}(p^4)$ one then obtains

$$\begin{aligned} M_N &= M_0 - 4c_1 m_\pi^2 - \frac{3g_A^2}{32\pi f_\pi^2} m_\pi^3 \\ &+ \left[e_1^r(\lambda) - \frac{3}{64\pi^2 f_\pi^2} \left(\frac{g_A^2}{M_0} - \frac{c_2}{2} \right) - \frac{3}{32\pi^2 f_\pi^2} \left(\frac{g_A^2}{M_0} - 8c_1 + c_2 + 4c_3 \right) \ln \frac{m_\pi}{\lambda} \right] m_\pi^4 \\ &+ \frac{3g_A^2}{256\pi f_\pi^2 M_0^2} m_\pi^5 + \mathcal{O}(m_\pi^6), \end{aligned} \quad (9)$$

where now

$$e_1 = e_1^r(\lambda) + \frac{3L(\lambda)}{2f_\pi^2} \left(\frac{g_A^2}{M_0} - 8c_1 + c_2 + 4c_3 \right).$$

We note that this expression includes the constants c_2 and c_3 which encode the influence of the Δ resonance in low energy pion-nucleon scattering. We further note that the terms up to m_π^4 have already been discussed in [15]. It is also interesting to observe that our truncation of the relativistic result at m_π^6 as shown in Eq.(9) formally coincides with the expansion of nucleon mass in HBChPT to fifth order, as there are no genuine 2-loop graphs at this order in the chiral expansion [16].

Having specified the general chiral results up to NNLO, we now proceed to confront these formulae with actual lattice data.

³In the next section we will demonstrate that numerically this truncation approximates the full function reasonably well for the parameter ranges considered here.

3 Numerical analysis and contact with lattice QCD

We proceed to discuss the numerical evaluation of Eqs.(7) and (9). We set the nucleon axial vector coupling and the pion decay constant equal to their physical values, $g_A = 1.267$ and $f_\pi = 92.4$ MeV. Strictly speaking, these quantities should be taken in the chiral limit. We have checked that using current estimates for g_A^0 and f_π^0 at $m_\pi \rightarrow 0$ [5, 17] does not lead to any significant changes in our final results. Without loss of generality we choose $\lambda = 1$ GeV. At order p^3 we are left with three unknown parameters (M_0 , c_1 and $e_1^r(1\text{GeV}) \equiv \hat{e}_1$) and four parameters at order p^4 (M_0 , c_1 , $A \equiv e_1^r(1\text{GeV}) + 3c_2/(128\pi^2 f_\pi^2)$ and $B \equiv c_2 + 4c_3$). Our NNLO result is identified with Eq.(9). This limits the number of tunable coefficients but still keeps sufficiently many orders in m_π such that the convergence of the expansion can be examined.

The unknown parameters are determined using a combined set of lattice QCD data obtained by the CP-PACS [8], JLQCD [9] and QCDSF [10] collaborations. These computations are performed using fully dynamical quarks with two light flavors. In order to minimize artifacts from discretization and finite volume effects, we have selected from the whole set of available data those with lattice spacings $a < 0.15$ fm and $m_\pi La > 5$. We also restrict ourselves to the data with $m_\pi < 800$ MeV with equal valence and sea quark masses, $m_{\text{sea}} = m_{\text{val}}$. A study of finite volume dependence is in preparation [18].

The fitting procedure for both the NLO and NNLO cases started from the minimal set of lattice data points with the smallest pion masses sufficient to determine the unknown coefficients. Then we successively added points with larger pion masses one by one and checked at each such cycle the stability of the fit, examining whether the output values agree with those of the previous one within error bars. This procedure works up to the inclusion of all 12 points compatible with the previous cuts. So we have chosen to fit all these data, in the range $520\text{ MeV} < m_\pi < 780\text{ MeV}$.

Successive steps in our analysis are summarized in table 1. In the first step we have fitted the whole set of lattice data using the $\mathcal{O}(p^3)$ result, Eq.(7) (Fit I), omitting the physical mass point. The result of this fit is consistent with that obtained when including the physical point as an additional input (Fit II, see also Fig.2). In this latter case, of course, the errors of M_0 and c_1 are much reduced as compared to Fit I. The pion-nucleon low-energy constants come of natural size. Furthermore, c_1 which determines the slope of $M_N(m_\pi^2)$ for small m_π^2 has the correct sign. The value of \hat{e}_1 is within the range quoted in ref.[3].

Once the unknown parameters are fixed, we can examine the LO and NLO corrections to the nucleon mass as m_π increases. For $m_\pi < 400$ MeV the NLO contribution is less than 50% of the LO correction (the leading linear growth of M_N with respect to m_q). Even for $m_\pi = 800$ MeV the NLO contribution does not exceed about 60% of the latter. Of course, *a priori* one should not assign much significance to extending the extrapolations to such exceedingly large values of the pion mass, close to the characteristic 1 GeV scale of spontaneous chiral symmetry breaking. But even fitting only a small number of points at the lowest available m_π , the resulting extrapolation curves still reproduce the lattice data at much larger pion masses very well. For example, fitting the four lattice data with $m_\pi < 600$ MeV and including the physical point as a constraint one obtains $M_0 = 0.891 \pm 0.002$ GeV,

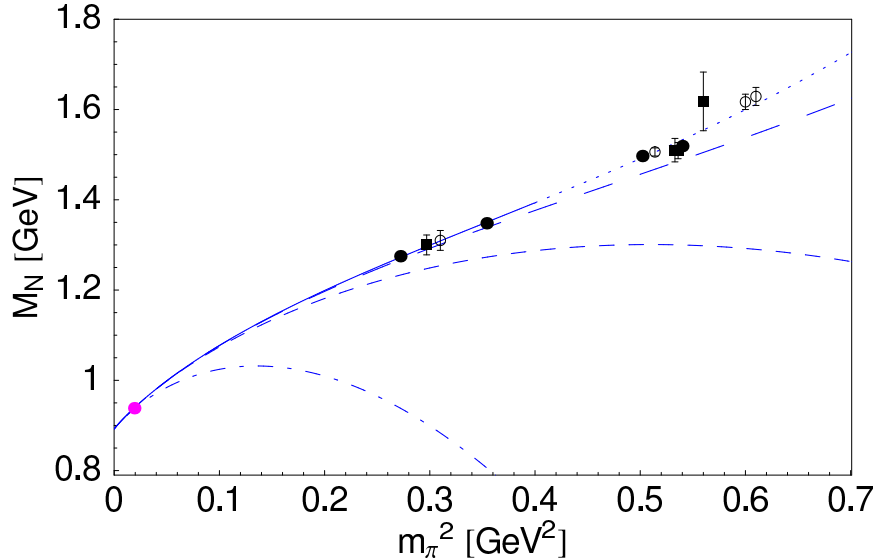


Figure 2: The solid/dotted line is the best fit curve using Eq.(7) and imposing the physical constraint (Fit II). The dotted extension of this curve for $m_\pi^2 > 0.4 \text{ GeV}^2$ just indicates the region where the application of the chiral expansion is usually believed to be potentially risky. The solid dots are CP-PACS data, the boxes refer to JLQCD and the empty circles to QCDSF. The dot-dashed, dashed and long-dashed curves show, respectively, the contributions from the sum of the first three, four and five terms in Eq.(8).

$c_1 = -0.79 \pm 0.03 \text{ GeV}^{-1}$, $\hat{e}_1 = 3.5 \pm 0.6 \text{ GeV}^{-3}$ and in addition a very good agreement with lattice data up to $m_\pi \approx 750 \text{ MeV}$, fully consistent with the complete Fit II.

Figure 2 also shows how the Fit II develops order by order in the pion mass when the full NLO expression (7) is expanded according to Eq.(8). The sizeable changes between the dash-dotted, short-dashed and long-dashed curve correspond to the large fluctuations reported in [2]. However, we remark again that all these contributions are of the same chiral order in the formulation of BChPT we use. We conclude that only the truncation at m_π^5 provides a decent approximation to our full $\mathcal{O}(p^3)$ result. Evidently, minor readjustments of parameters, consistent with Fit I within its errors, yield a successful interpolation even when the chiral expansion of the NLO result is truncated at order m_π^5 . For all these procedures, we find $\chi^2_{\text{d.o.f.}} < 1$.

For the NNLO case represented by Eq.(9), fitting the whole set of 12 lattice points and setting reasonable starting ranges in the MINUIT routine for M_0 (between 0.85 and 0.95 GeV) and c_1 (between -1.0 and -0.6 GeV^{-1}), we find the results displayed as Fit III in table 1 ($\chi^2_{\text{d.o.f.}} = 0.62$). In Fit IV we have also included the physical nucleon mass point. The resulting estimates for c_1 are perfectly consistent with the value determined by Becher and Leutwyler in their analysis of low-energy πN scattering in $SU(2)_f$ relativistic BChPT [19]. They are also in agreement with ref.[20]. The low-energy constants c_2 and c_3 cannot be extracted separately; only their combination in the form $c_2 + 4c_3$ enters. The value for this

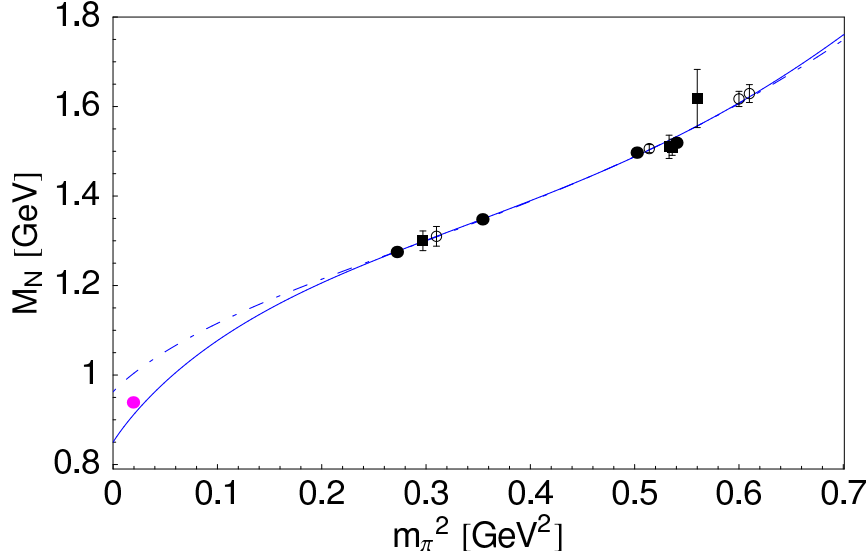


Figure 3: Best fit curves for the unconstrained NLO-Fit I (dot-dashed) and NNLO-Fit III (solid).

combination found in Fits III and IV deserves a brief discussion. We recall that the NNLO analysis of the isospin-even pion-nucleon s-wave scattering length and isospin-averaged p-wave scattering volume constrains these constants, as follows. The approximate vanishing of the isospin-even scattering length at threshold implies $c_2 + c_3 - 2c_1 - g_A^2/(8M_N) \approx 0$. The isospin averaged scattering volume is dominated by the $\Delta(1232)$ contribution. Its empirical value suggests $c_3 \simeq -4 \text{ GeV}^{-1}$. Given $c_1 \simeq -0.9 \text{ GeV}^{-1}$, we observe that our estimate, $c_2 + 4c_3 \approx -(10 \pm 2) \text{ GeV}^{-1}$ is indeed roughly consistent with such constraints. One notes, however, that there is a tendency toward magnitudes of c_3 which are smaller than those quoted in [20].

From direct comparison of the extrapolation curves in Fig.3 we can see that corrections at order p^4 are quite small with respect to the $\mathcal{O}(p^3)$ result for the whole range in m_π we analyzed.

3.1 The sigma term of the nucleon

The pion-nucleon sigma term σ_N , Eq.(4), translates into

$$\sigma_N = m_\pi^2 \frac{\partial M_N}{\partial m_\pi^2} , \quad (10)$$

if we assume that the Gell-Mann - Oakes - Renner (GOR) relation $m_\pi^2 \sim m_q$ holds and we can neglect $\mathcal{O}(m_q^2)$ terms. Empirical constraints on these terms by an improved analysis of s-wave $\pi\pi$ scattering lengths [21] do indicate that the $\mathcal{O}(m_q^2)$ corrections to the GOR relation are very small, although this statement becomes progressively less accurate with

increasing quark masses, and further detailed examination of the role of strange quarks in this context is necessary. A recent systematic analysis [22] of results for pseudo-Goldstone boson masses from $N_f = 2$ lattice QCD comes to conclusions consistent with those drawn in ref.[21]. We therefore use Eq.(10) in the following.

At p^3 level starting from Eq.(8) one gets the expression

$$\begin{aligned}\sigma_N &= -4c_1 m_\pi^2 - \frac{9g_A^2}{64\pi f_\pi^2} m_\pi^3 \\ &+ 2e_1^r(\lambda) m_\pi^4 - \frac{3g_A^2}{64\pi^2 f_\pi^2 M_0} (3 + 4 \ln \frac{m_\pi}{\lambda}) m_\pi^4 \\ &+ \frac{15g_A^2}{512\pi f_\pi^2 M_0^2} m_\pi^5 + \mathcal{O}(m_\pi^6).\end{aligned}\quad (11)$$

The corresponding NNLO result is derived from Eq.(9):

$$\begin{aligned}\sigma_N &= -4c_1 m_\pi^2 - \frac{9g_A^2}{64\pi f_\pi^2} m_\pi^3 \\ &+ \left[2e_1^r(\lambda) - \frac{1}{16\pi^2 f_\pi^2} \left(\frac{9g_A^2}{4M_0} - 6c_1 + 3c_3 \right) - \frac{3}{16\pi^2 f_\pi^2} \left(\frac{g_A^2}{M_0} - 8c_1 + c_2 + 4c_3 \right) \ln \frac{m_\pi}{\lambda} \right] m_\pi^4 \\ &+ \frac{15g_A^2}{512\pi f_\pi^2 M_0^2} m_\pi^5 + \mathcal{O}(m_\pi^6).\end{aligned}\quad (12)$$

Our deduced values of σ_N at the physical point are summarized in table 2. The behaviour of the sigma term as a function of the pion mass is shown in Fig.4. Within errors, this curve is compatible with the "empirical" sigma term $\sigma_N = 45 \pm 8$ MeV extracted in ref.[23], but it does not favor the much larger value reported in ref.[24]. Our result is also consistent with the analysis of ref.[25], within the larger uncertainties quoted there.

4 Discussion and conclusions

The present work has been aimed at improving and updating interpolations of the nucleon mass, using chiral effective field theory, between the range of relatively large quark masses accessible in full lattice QCD simulations, and the small quark masses relevant for comparison with physical observables. A remarkably good extrapolation can already be achieved at p^3 level using relativistic BChPT. In either case short distance dynamics, including effects of the $\Delta(1230)$ and possibly other resonance excitations of the nucleon, are encoded in a single counter term that controls the contributions of order m_π^4 . $\mathcal{O}(p^3)$ relativistic BChPT is therefore free of limitations of HBChPT discussed in [2, 3]. Apart from the nucleon mass in the chiral limit, the only remaining parameter, c_1 , drives the pion-nucleon sigma term. Our extrapolation is based on a selected set of lattice data corresponding to the largest available lattice volumes and the lowest available pion masses, in order to minimize uncertainties from finite size effects and from quark masses too large to be handled using perturbative

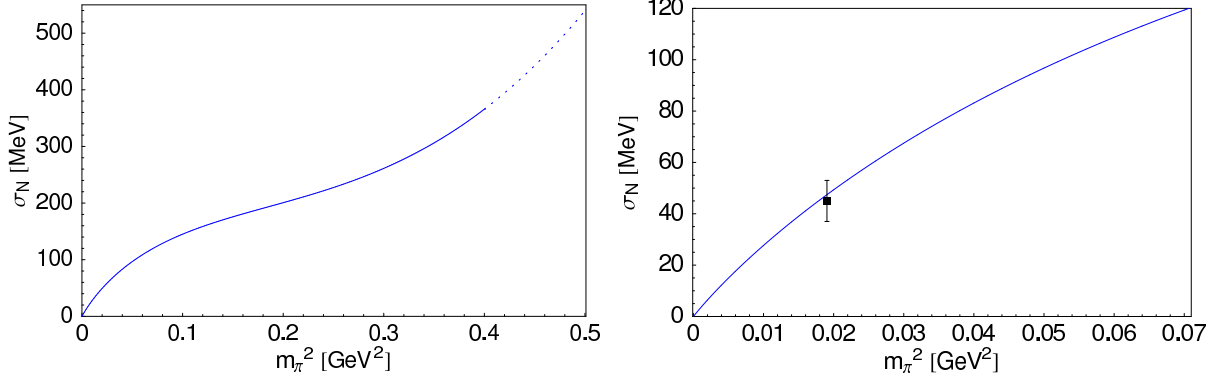


Figure 4: Pion-nucleon sigma term as a function of m_π^2 from Eq.12, using central values from Fit IV. The small m_π region is magnified in the right panel and plotted together with the frequently quoted empirical $\sigma_N = 45 \pm 8$ MeV [23].

chiral expansions. Surprisingly, the resulting extrapolations work even in a pion mass region where the approach is commonly believed to become less reliable.

The extension to NNLO, truncated at order m_π^5 , introduces in addition the pion-nucleon low-energy constants $c_{2,3}$ which primarily reflect the impact of Δ resonance physics on low-energy πN dynamics. The optimal fit interpolating the nucleon mass between the chiral limit and the lattice data remains remarkably stable and even improves slightly when going from NLO to NNLO (see Table 1). The resulting "best fit" value of the combination $c_2 + 4c_3$ entering in the m_π^4 term has the correct sign and is close in magnitude to empirical determinations, although it tends to prefer values of c_3 somewhat smaller than those quoted in the literature.

An interesting observation is that the differences between extrapolations with or without inclusion of the physical nucleon mass point as a constraint are quite small. The band of M_N values at the physical pion mass, "predicted" with an uncertainty of less than 10% by the NNLO extrapolation based entirely on the lattice data (cf. Fit III), encloses the empirical M_N within errors. In fact the central value of $M_N = M_0 + \sigma_N$ obtained in this extrapolation misses the empirical nucleon mass (from below) by less than 5%. We find $M_N = 910 \pm 70$ MeV at the physical value of the pion mass. There is an interesting side aspect to this observation. Given that this result is obtained from $N_f = 2$ lattice QCD excluding strange quarks, this may indicate that the contribution of strange sea quarks to the nucleon mass is relatively small, in qualitative agreement with ref.[12] but at variance with many other suggestions of large strange quark admixtures to M_N .

The pion-nucleon sigma term deduced from the m_π dependence of the nucleon mass in the NNLO "best fit" (Fit IV) is fully consistent with that obtained by Gasser, Leutwyler and Sainio [23]. This is a nontrivial result since no such constraint has been built into the procedure.

In summary, the outcome of the present study is promising. It demonstrates that extrapolation methods based on chiral effective field theory can be successfully combined with

Table 1: Fit results for $M_N(m_\pi)$ described in detail in the text. Fit I refers to the extrapolation based on the NLO result, Eq.(7). Fit II includes the physical nucleon mass as additional constraint. Fit III and Fit IV are based on the NNLO result, Eq.(9), with and without respectively including the physical value of M_N as a constraint.

	M_0 [GeV]	c_1 [GeV $^{-1}$]	\hat{e}_1 [GeV $^{-3}$]	A [GeV $^{-3}$]	B [GeV $^{-1}$]
Fit I	0.96 ± 0.08	-0.7 ± 0.1	4.2 ± 0.6	-	-
Fit II	0.892 ± 0.001	-0.77 ± 0.01	3.7 ± 0.1	-	-
Fit III	0.85 ± 0.07	-0.97 ± 0.08	-	3.4 ± 0.2	-10.5 ± 2
Fit IV	0.885 ± 0.006	-0.89 ± 0.02	-	3.7 ± 0.2	-9.5 ± 2

Table 2: The pion-nucleon sigma term deduced from the NLO and NNLO fits for $M_N(m_\pi)$ given in Table 1.

	σ_N [MeV]
Fit I	35 ± 8
Fit II	41 ± 1
Fit III	53 ± 8
Fit IV	47 ± 3

lattice QCD results in order to bridge the gap between simulations and observables. Of course, remaining uncertainties need to be further investigated, such as corrections due to finite lattice volume and questions concerning convergence properties of the chiral expansion with quark masses exceeding 100 MeV.

We gratefully acknowledge many stimulating discussions with M. Göckeler, G. Schierholz and A. Thomas. We thank the QCDSF-UKQCD Collaboration for providing us with their data prior to publication.

References

- [1] A.W. Thomas and W. Weise, The Structure of the Nucleon, Wiley-VCH, Berlin (2001), and references therein.
- [2] R.D. Young, D.B. Leinweber and A.W. Thomas, [[hep-lat/0212021](#)].
- [3] V. Bernard, T.R. Hemmert and U.-G. Meißner, [[hep-ph/0307115](#)].
- [4] D.B. Leinweber, A.W. Thomas, K. Tsushima and S.V. Wright, Phys. Rev. **D61**, 074502 (2000); D.B. Leinweber, A.W. Thomas and R.D. Young, [[hep-lat/0302020](#)].
- [5] T.R. Hemmert and W. Weise, Eur. Phys. J. **A15**, 487 (2002); T.R. Hemmert, M. Procura and W. Weise, Nucl. Phys. **A721**, 938c (2003) and [[hep-lat/0303002](#)], Phys. Rev. D, in print.
- [6] M. Göckeler et al., [[hep-lat/0303019](#)]; J.D. Ashley, D.B. Leinweber, A.W. Thomas and R.D. Young, [[hep-lat/0308024](#)].
- [7] W. Detmold et al., Phys. Rev. Lett. **87**, 172001 (2001).
- [8] CP-PACS Collaboration, A. Ali Khan et al., Phys Rev. **D65**, 054505 (2002); Erratum-ibid. **D67** 059901 (2003).
- [9] JLQCD Collaboration, S. Aoki et al., [[hep-lat/0212039](#)].
- [10] QCDSF-UKQCD Collaboration, G. Schierholz et al., private communication.
- [11] *e.g.* see J.F. Donoghue, E. Golowich and B.R. Holstein, Dynamics of the Standard Model, Cambridge University Press, Cambridge (1992).
- [12] X. Ji, Phys. Rev. Lett. **74**, 1071 (1995).
- [13] T. Becher and H. Leutwyler, Eur. Phys. J. **C9**, 643 (1999).
- [14] N. Fettes, U.-G. Meißner, M. Mojžiš and S. Steininger, Annals Phys. **283**, 273 (2000); Erratum-ibid. **288**, 249 (2001).
- [15] J. Gasser, M.E. Sainio and A. Svarc, Nucl. Phys. **B307**, 779 (1988).
- [16] J.A. McGovern and M.C. Birse, Phys Lett. **B446**, 300 (1999).
- [17] P. Gerber and H. Leutwyler, Nucl. Phys. **B321**, 387 (1989).
- [18] A. Ali Khan et al., talk given at Lattice 2003, forthcoming.
- [19] T. Becher and H. Leutwyler, JHEP 0106, 017 (2001).
- [20] V. Bernard, N. Kaiser and U.-G. Meißner, Nucl. Phys. **A615**, 483 (1997).

- [21] G. Colangelo, J. Gasser and H. Leutwyler , Nucl. Phys. **B603**, 125 (2001) and Phys. Rev. Lett. **86**, 5008 (2001).
- [22] S. Dürr, [hep-lat/0208051], March 2003.
- [23] J. Gasser, H. Leutwyler and M.E. Sainio, Phys. Lett. **B253**, 252 (1991).
- [24] M.M. Pavan, R.A. Arndt, I.I. Strakovsky and R.L. Workman, [hep-ph/0111066].
- [25] D.B. Leinweber, A.W. Thomas and S.V. Wright, Phys. Lett. **B482**, 109 (2000).